JOURNAL OF SOLID STATE CHEMISTRY 24, 189–197 (1978)

Mössbauer Effect Study of Carbides and Silico-Carbides. II. $(Mn_{1-x}Fe_x)_5SiC$

J. M. DUBOIS,* G. LE CAER,* AND J. P. SENATEUR†

*Laboratoire de Métallurgie associé au C.N.R.S. n° 159, Ecole des Mines, 54042 Nancy Cédex, France, and †Equipe de recherche n° 155, I.N.P.G., Section Génie Physique, B.P. 15, Centre de Tri 38040 Grenoble Cédex, France

Received May 18, 1977; in revised form September 26, 1977

The substitution of iron in Mn_5SiC has been studied by Mössbauer spectroscopy at room temperature. The Mn_3 site is the first saturated site while the filling of the Mn_4 site is the most difficult. The magnitude of the quadrupole splittings of iron atoms having two carbon nearest neighbors at a distance close to 2 Å in Fe_3C, Fe_5C_2, Mn_5SiC, and some $M_3M'C$ perovskite carbides in the paramagnetic state are discussed. These quadrupole splittings are practically insensitive to the metallic neighborhood of the sites under consideration. They increase regularly with the angle of the two iron–carbon bonds.

Introduction

Many carbides such as M_3C, M_5C_2, M_7C_3, M_5SiC, M_8Si_2C, where M is a transition metal atom chosen among (Cr, Mn, Fe, Co) possess a common structural element constituted by a trigonal prism of M atoms centered on a carbon atom. In a preceding paper (*1*) referred to as I, we have shown the similarities between the Mössbauer hyperfine parameters of Fe_3C and Fe_5C_2. In order to search for a common behavior of the hyperfine parameters of the carbides quoted above, we have undertaken a ^{57}Fe Mössbauer study of the solid solution $(Mn_{1-x}Fe_x)_5SiC$ which exists in the range $0 \leqslant x \leqslant 0.6$ (*2*).

We have investigated the iron substitution and the isomer shift and quadrupole splitting variations as a function of x at room temperature where these carbides are paramagnetic. The paramagnetic quadrupole splittings of iron atoms in Fe_3C, Fe_5C_2, in $(Mn_{1-x}Fe_x)_5SiC$, and in some cubic perovskite carbides are discussed.

Experimental Methods

The samples are obtained by solid state diffusion, between 800 and 1200°C, from a mixture of high purity elements: Mn (99.9%), Fe (99.9%), Si (99.99%), C (99.99%) as described by Spinat (*2*). Mössbauer spectra of $(Mn_{1-x}Fe_x)_5SiC$ were obtained at room temperature for six values of x ranging from $x = 0.018$ (^{57}Fe enriched sample) to $x = 0.5$, with the help of a constant acceleration Elron Spectrometer. The Mössbauer spectra (400 channels, 10^6 counts per channel) have been analyzed by a least-squares computer program assuming Lorentzian shapes and assuming that the two peaks belonging to a doublet have equal widths and amplitudes.

Crystallographic Structure and Magnetic Properties of $(Mn_{1-x}Fe_x)_5SiC$

Mn_5SiC is an orthorhombic carbide (spatial group $Cmc2_1$) with lattice parameters $a = (10.198 \pm 0.001)$ Å, $b = (8.035 \pm 0.001)$ Å, $c = (7.630 \pm 0.001)$ Å (*2*). The structure

0022-4596/78/0242-0189 $02.00/0

has been determined by Spinat and Herpin from X-ray (*2*) and neutron diffraction (*3*) studies. It can be described by a set of planes, perpendicular to the [100] direction, containing Mn, Mn–C, Si, Mn, ..., atoms, respectively. The manganese sites are respectively Mn_1, Mn_3, Mn_4, Mn_5 (eight atoms in the general position per unit cell) and Mn_2, Mn_2^* (four atoms in the special position). The metal atom lattice can be described by a chain of A and B octahedra (Fig. 1). These A and B octahedra are formed from ($2Mn_1$, $2Mn_5$, $2Mn_2$) and ($2Mn_1$, $2Mn_5$, Mn_2, Mn_2^*), respectively. Neutron diffraction (*3*) shows that carbon atoms (C and C*) are located at the centers of trigonal prisms P analogous to the ones found in M_3C, M_5C_2, and M_7C_3 type carbides (Fig. 1).

The coordination numbers C.N. of the manganese atoms are 11 for Mn_3 and Mn_4, 12 for Mn_2 and Mn_2^*, 14 for Mn_1 and Mn_5. From their neutron diffraction results, Spinat and Herpin (*3*) have shown that the elements, whose atomic radii are less than that of manganese, substitute preferentially into the sites of lowest coordination. The Mn_3 and Mn_4 sites are totally substituted in $(Mn_{0.5}Fe_{0.5})_5SiC$ while the Mn_2 and Mn_2^* are only partially

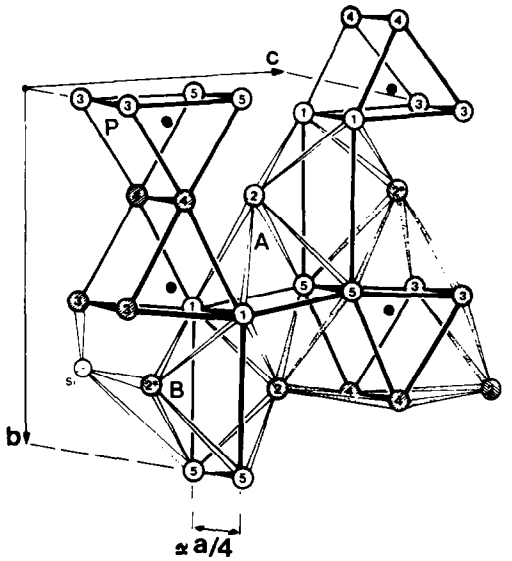

FIG. 1. Crystal structure of Mn_5SiC.

TABLE I

MÖSSBAUER EFFECT STUDY OF THE Mn–Fe SUBSTITUTION AT ROOM TEMPERATURE

Crystallographic site	C.N.	Mn–C distances (Å)		Mn–Si distances (Å)	
Mn_3	11	2.00	4.03	2.39	4.04
		2.06	4.07	(2)	4.12
Mn_4	11	2.02	3.84	2.34	3.45
		2.05	4.00	2.46	4.11
Mn_2	12	2.51	3.58	2.54	2.72
		2.79	3.60	(2)	(2)
Mn_2^*	12	2.18	3.07	2.62	4.91(2)
		2.32	3.16	(2)	4.92(2)

substituted. The filling of these last four sites corresponds to the solid solution limit $x = 0.6$. These authors have proposed that, starting from $x = 0$, the Mn_3 and Mn_4 sites are first substituted and that the Mn_2 and Mn_2^* are later simultaneously substituted.

Table I gives the Mn–C and Mn–Si distances for the sites of lowest C.N. These distances decrease with x (*3*). We finally note that the Mn_3 and Mn_4 sites are similar to the Fe_{II} site of cementite.

Spinat (*3*) has shown that Mn_5SiC is magnetic with a Curie temperature of (284 ± 1)°K. The determination of the manganese magnetic moment is difficult: at 20°K under 26.6 kOe, the measured moment is 0.35 μ_B per Mn atom but the saturation of the magnetization is not reached under these conditions. The magnetic structure is complex. It can be described by both an antiferromagnetic and a helimagnetic sublattice. When iron is substituted for manganese, the Curie temperature first decreases from $x = 0$ to $x \simeq 0.43$ ($T_c < 77$°K) and then increases up to $T_c = (183 \pm 2)$°K for $x = 0.6$.

Mössbauer Effect Study of the Mn–Fe Substitution at Room Temperature

Figure 2 shows the Mössbauer spectra of $(Mn_{1-x}Fe_x)_5SiC$, at room temperature, for $x = 0.018$ (^{57}Fe), 0.1, 0.2, 0.3, 0.4, and 0.5.

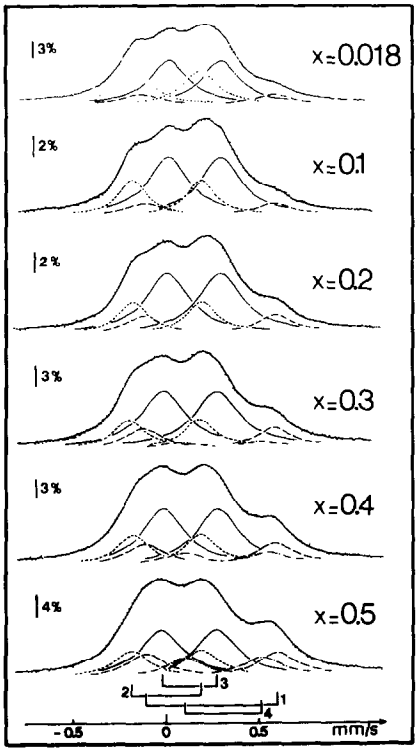

FIG. 2. Mössbauer spectra of $(Mn_{1-x}Fe_x)_5SiC$ at room temperature.

The first spectrum ($x = 0.018$) shows that at least three iron sites exist from the lowest iron contents on. We have calculated the experimental spectra with the help of three symmetric doublets 1, 2, and 3. The only satisfying combinations of these doublets are shown in the first column of Table II and the $X^2(x)$ values for 400 experimental points are given.

The second combination is clearly the best one. This conclusion will be further confirmed in the discussion. As, at least for $x = 0.5$, the four sites Mn_3, Mn_4, Mn_2, and Mn_2^* are known to be substituted (*3*), we have performed a second calculation with four doublets 1, 2, 3, 4. The quadrupole splittings of sites 1, 2, 3 do not significantly vary with x (Table III) and have been used in the second fitting. The results are given in the last line of Table II. The amplitude of the fourth doublet is only significant for the three highest iron contents (Fig. 4).

The number n_i (x) of iron atoms in site i is deduced from

$$n_i(x) = 5x\left(\frac{A_i/f_i}{\sum_{k=1}^{4}(A_k/f_k)}\right), \tag{1}$$

where A_k is the area of the kth doublet and f_k the corresponding Debye–Waller factor. The structure imposes the following restrictions on the $n_i(x)$ values:

$$\begin{aligned} &n_{Mn_2}(x),\ n_{Mn_2^*}(x) \leqslant 0.5, \\ &n_{Mn_3}(x),\ n_{Mn_4}(x) \leqslant 1. \end{aligned} \tag{2}$$

To obtain an order of magnitude of the mean Debye–Waller factors of the Mn_2, Mn_2^*, Mn_3, Mn_4 sites, we have used the anisotropic temperature factors determined by Spinat *et*

TABLE II

x	0.018	0.1	0.2	0.3	0.4	0.5
3 2 1	527	556	912	563	1064	1289
3 2 1	497	309	270	287	283	341
3 2 1 4	497	309	270	278	301	337

0 mm/sec

TABLE III

	Doublet no.	Site	0.018	0.10	0.20	0.30	0.40	0.50
Δ (mm/sec) ± 0.01	1	Mn_2^*	0.71	0.70	0.71	0.72	0.71	0.70
	2	Mn_4	0.36	0.36	0.37	0.38	0.37	0.37
	3	Mn_3	0.28	0.28	0.29	0.29	0.29	0.29
	4	Mn_2	—	—	—	0.44	0.46	0.42
δ (mm/sec) ± 0.01	1	Mn_2^*	0.22	0.23	0.23	0.24	0.24	0.24
	2	Mn_4	0.	0.	0.	0.	0.01	0.
	3	Mn_3	0.15	0.15	0.14	0.14	0.14	0.12
	4	Mn_2	—	—	—	0.30	0.33	0.31
Γ (mm/sec) ± 0.01	1	Mn_2^*	0.26	0.24	0.22	0.22	0.25	0.25
	2	Mn_4	0.23	0.21	0.21	0.21	0.23	0.24
	3	Mn_3	0.25	0.27	0.28	0.28	0.27	0.28
	4	Mn_2	—	—	—	0.22	0.25	0.25
n ± 0.02	1	Mn_2^*	0.01	0.05	0.14	0.22	0.34	0.49
			(0.02)	(0.06)	(0.15)	(0.24)	(0.35)	(0.50)
	2	Mn_4	0.03	0.13	0.23	0.30	0.43	0.53
			(0.03)	(0.14)	(0.24)	(0.32)	(0.45)	(0.54)
	3	Mn_3	0.05	0.32	0.63	0.92	1.04	1.09
			(0.04)	(0.30)	(0.61)	(0.88)	(0.98)	(1.01)
	4	Mn_2	—	—	—	0.06	0.19	0.39
						(0.06)	(0.22)	(0.45)

al. (*2*, *4*) by X-ray diffraction. These factors allow us to calculate the mean-square displacement $\langle X^2 \rangle$ along any direction (*5*). Weighted means of $f = \exp\{-\langle X^2 \rangle / \lambda\bar{}^2\}$ are finally deduced for a random powder sample ($\lambda\bar{} = \lambda/2\pi$, where λ is the wavelength of the 14.4-keV radiation). This calculation gives the following Debye–Waller factors (normalized with respect to the largest factor):

$$f_{Mn_2} = 0.8, \qquad f_{Mn_2^*} = f_{Mn_4} = 0.9, \qquad f_{Mn_3} = 1, \tag{3}$$

and shows that the amplitudes of the two peaks of each doublet are equal within less than 1%.

The values $n_i(x)$ (Eq. 1) are given in Table III for $f_1 = f_2 = f_3 = f_4 = 1$. For $x = 0.50$, relations (2) show that the doublets 2 and 3 correspond to the Mn_3 and Mn_4 sites (this assignment is in fact sufficient for the discussion of the quadrupole splittings). As n_3 must be less than or equal to 1, we deduce that the Debye–Waller factors f_2 and f_3 must be different and that $f_2 < f_3$. From Eq. (3), we then attribute the doublets 2 and 3 to the Mn_4 and Mn_3 sites, respectively.

The extrapolation of $n_1(x)$, for $x = 0.4$, to $x = 0.6$ (Fig. 4) gives $n_1\ (0.6) = 0.5$ in agreement with relations 2. The first two n_4 values are also aligned with the point ($x = 0.6$, $n_4 = 0.5$) (Fig. 4). This further confirms our attribution of the doublets 2 and 3 to the Mn_4 and Mn_3 sites.

Spinat and Herpin (*3*) have determined the atomic positions for $x = 0.5$. The reliability factor is, however, two times greater than that found for Mn_5SiC. Nevertheless, this determination shows that the distances between an atom occupying the Mn_2, Mn_2^*, Mn_3 crystallographic sites and its nearest neighbors decrease faster with x than those of the Mn_4 site. This may explain that it is difficult to fill the Mn_4 site (Fig. 4) and that it becomes more and more difficult to prepare the $(Mn_{1-x}Fe_x)_5SiC$ solid solution when x becomes increasingly larger and practically impossible to reach the $x = 0.6$ limit (*3*).

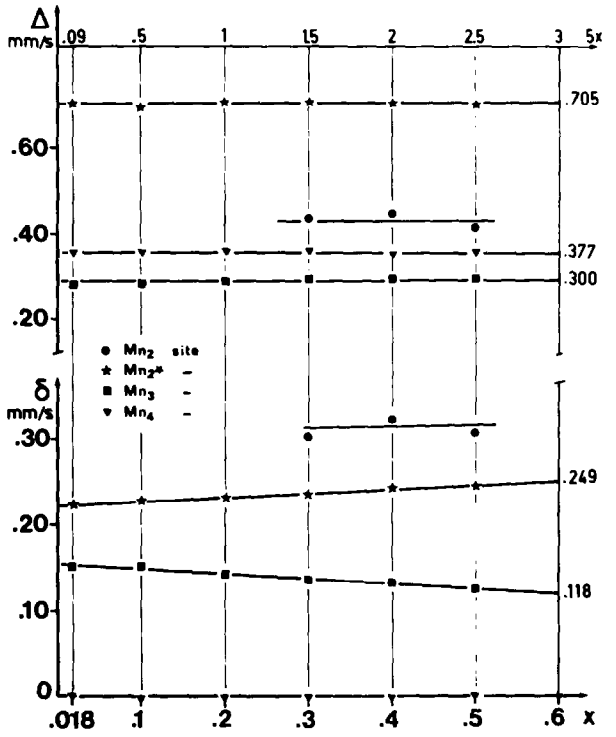

FIG. 3. Quadrupole splittings and isomer shifts of the various sites, as a function of x, in $(Mn_{1-x}Fe_x)_5SiC$ at room temperature.

We then assume that iron substitutes preferentially among the sites of lowest C.N. into those offering the smallest volume. We so attribute the doublet 1 to the Mn_2^* site and the doublet 4 to the Mn_2 site. We will later see that this scheme provides a coherent description of the quadrupole splittings of these sites.

Table III gives the quadrupole splittings Δ, the isomer shifts δ with respect to metallic iron at room temperature, the widths Γ of each doublet and the number n of iron atoms per site, calculated from $f_1 = f_2 = f_3 = f_4 = 1$ and from Eq. (3) (numbers between brackets).

The $\Delta(x)$, $\delta(x)$ curves are plotted on Fig. 3, the values $\Delta(0.6)$ and $\delta(0.6)$ for the various sites, deduced from a linear fitting, are also indicated. Mössbauer spectra were also obtained at 190°K for $x = 0.3$, 0.4, 0.5. They lead to quadrupole splittings identical to those of Table III. The $n(x)$ curves are shown on Fig. 4. These curves are practically linear for $x \leqslant 0.4$ ($x \leqslant 0.3$ for n_{Mn_3}). the Mn_3 site filling is the fastest and this site is saturated around $x = 0.43$.

In conclusion, the present study shows that iron atoms are substituted into three sites, instead of two as postulated by Spinat and Herpin (*3*), from the lowest iron contents on. Our results, for $x = 0.5$, agree with those of the last authors with the restriction that the Mn_3

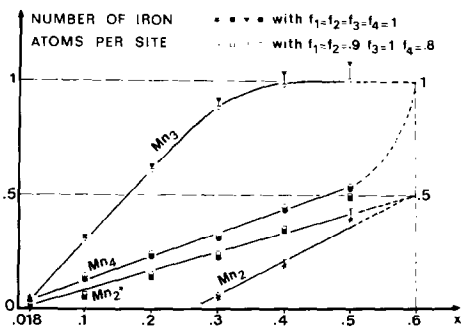

FIG. 4. Iron substitution in $(Mn_{1-x}Fe_x)_5SiC$ as a function of x.

and Mn_4 sites are not equally occupied. When x increases, the local distortions favor the filling of new sites, for example, the Mn_2 site above $x \simeq 0.25$. The Mn_4 site's distortions are weaker and explain the difficulty in filling this site.

Discussion

We will essentially discuss the hyperfine parameters of cementite type and related carbides in the paramagnetic state.

The Mn_3 and Mn_4 sites of Mn_5SiC are similar to the Fe_{II} site of Fe_3C and Fe_5C_2. The coordinations are the same as are approximately the metal–metal and metal–carbon distances. However, the presence of silicon in the neighborhood of iron atoms needs to be considered. The quadrupole splittings are, in absolute value, 0.32, 0.37 (*1*), 0.28, 0.36 mm/sec for the Fe_{II} site of Fe_3C and Fe_5C_2 and Fe in the Mn_3, Mn_4 sites of Mn_5SiC, respectively.

As already noted by Fruchart (*6*), the cementite type and related carbides all show short metal–carbon distances of the order of 2 Å. This reveals the existence of strong metal–carbon bonds which are responsible for the cohesion of the trigonal prism encountered in all these structures. From the rapid variation of the function $1/r^3$, where r is an electron–nucleus distance, the electrons which participate in these strong bonds are expected to give the major contribution to the quadrupole splittings measured at the iron nucleus. In order to test this hypothesis, we will consider the absolute values Δ of the quadrupole splittings of iron atoms having two carbon nearest neighbors at a distance close to 2 Å in cementite type and related carbides in the paramagnetic state. Such atoms also exist in various cubic perovskite carbides $M_3M'C$ (M = Fe or Mn, M' = Al, Ga, Ge, Zn, Sn) (*7*, *8*) and will be included. Although such iron atoms are also encountered in ε carbide (*9*) or in splat-quenched Fe–C and Fe–C–Si ε phases (*10*), they will not be considered because it is difficult to know their quadrupole splittings in these metastable and nonstoichiometric phases. The effect of the next nearest neighbors, generally situated at much greater distances, will also be discussed. We will first show that the quadrupole splittings are practically insensitive to the metallic neighborhood of the iron atoms under consideration.

1. *Fe_3C-Type Carbides*

Table IV summarizes the various experimental results, Δ_I and Δ_{II} being the absolute values of the quadrupole splittings of Fe_I and Fe_{II}, respectively.

The indexing of the Fe_3C Mössbauer spectra made by Huffman *et al.* (*11*) leads to an isomer shift difference $\Delta\delta = \delta_{II} - \delta_I = (0.17 \pm 0.01)$ mm/sec above the Curie temperature T_c while, below T_c, $\Delta\delta$ is known to be zero within experimental uncertainties (*1*, *12*). As so large a discontinuity in $\Delta\delta$ is not expected, we have recalculated Δ_I and Δ_{II} from the data of these authors using our indexing

TABLE IV

Compound	Δ_I (mm/sec)	Δ_{II} (mm/sec)	Reference
Fe_3C	0.68 ± 0.03	0.32 ± 0.01	(*1*)
	0.65 ± 0.02	0.31 ± 0.02	(*11*)[a]
	0.58 ± 0.04	0.32 ± 0.04	(*12*)
$(Fe_{1-x}Cr_x)_3C$, $0 \leqslant x \leqslant 0.245$	Experimental data fitted with only one quadrupole doublet, $\Delta \simeq 0.4$–0.5 mm/sec		(*13*)
$(Fe_{1-x}Mn_x)_3C$, $0 \leqslant x \leqslant 0.60$	0.66 ± 0.01	0.33 ± 0.02	(*11*)[a]

[a] Recalculated values.

(*1*) which gives $\Delta\delta = (-0.03 \pm 0.03)$ mm/sec above T_c. The recalculated values agree well with ours. Finally, the donor theory (*11*) cannot contribute to the correct indexing of the peaks because this theory cannot interpret both the isomer shifts and the hyperfine fields of the Fe_I and Fe_{II} atoms.

The quadrupole splittings are independent of x in $(Fe_{1-x}Mn_x)_3C$. The same is true in $(Fe_{1-x}Cr_x)_3C$ from the results of Shigematsu (*13*) in spite of oversimplified Mössbauer spectra fittings. The Δ values obtained by the last author agree with the Δ value (0.45 ± 0.06 mm/sec) found by Maksimov *et al.* (*14*) in Fe_3C from the same simplified analysis. $(Fe_{1-x}Cr_x)_3C$ carbides have also been studied by Kuzmann *et al.* (*15*). However, their paper does not give the hyperfine parameters deducted from the fittings.

Simple point-charge calculations also show that the metallic contribution to the total lattice electric field gradient is less than 10% for Fe_I and Fe_{II}. Although little is known about the temperature variations of the quadrupole splittings, we note that the same Δ values are measured for Fe_3C at 551°K (*1*) and for $(Fe_{1-x}Mn_x)_3C$ ($x \geqslant 0.010$) at room temperature. We have calculated the iron–carbon and iron–iron distances with the help of the atomic positions and lattice parameters determined by Fasiska and Jeffrey (*16*). Our results agree with theirs, except for the number of carbon nearest neighbors of Fe_{II}. They have found three Fe_{II}–C distances of 2.04 Å while we have found only two. The Fe_I atom has a third carbon neighbor at 2.85 Å. Its influence is certainly much less than the one of the two carbons at 1.97 and 1.99 Å. On the contrary, the Fe_{II} atom has a third carbon neighbor at 2.37 Å which may be responsible for a larger part of the total quadrupole splitting.

2. *Fe_5C_2-Type Carbides*

The Fe_{III} atom which has four carbon atom neighbors at 2.07 Å will not be considered. The Δ_I and Δ_{II} quadrupole splittings are also independent of x in $(Fe_{1-x}Mn_x)_5C_2$ (Table V).

The indexing of Huffman *et al.* (*11*) has also been shown (*1*) to lead to too great an isomer shift difference variation at the Curie temperature. The recalculated values, using the indexing of paper I, also agree with ours. The last remarks made for Fe_3C are also valid for Fe_5C_2.

3. *$(Mn_{1-x}Fe_x)_5SiC$*

The quadrupole splittings are independent of x (Fig. 3). Only minor differences in the Mn–Si distances for the Mn_3 and Mn_4 sites (Table I) produce a strong variation of their isomer shifts (Table III) while the quadrupole splittings are nearly the same. The assumption that silicon modifies mainly the number of iron 4*s* electrons, is consistent with the experimental observations. In this case, silicon would only slightly affect the quadrupole splittings. This may explain the similarities between the quadrupole splittings of the Fe_{II} (Fe_3C, Fe_5C_2) and Mn_3, Mn_4 sites. The same effect is observed in β-$FeSi_2$ (*17*). In this compound the two iron sites are nearly identical. The Fe–Si distances are distributed in the range 2.34–2.39 Å for one site and 2.33–2.44 Å for the other. The quadrupole splittings are the same

TABLE V

Compound	Δ_I (mm/sec)	Δ_{II} (mm/sec)	Reference
Fe_5C_2	0.79 ± 0.02	0.37 ± 0.02	(*1*)
$(Fe_{2.5}Mn_{2.5})C_2$	0.81 ± 0.02	0.37 ± 0.02	Unpublished results
$(Fe_{1.1}Mn_{3.9})C_2$	0.73 ± 0.02	0.38 ± 0.02	(*11*)[a]

[a] Recalculated values.

but the isomer shifts differ by 0.12 mm/sec. The Mn_2–C distances are greater than the Mn_2^*–C distances (Table I). This may account for a greater Mn_2^* quadrupole splitting. We note finally that the ratio of the quadrupole splittings of the Mn_2 and Mn_2^* is (1.6 ± 0.1) while the corresponding ratio, to the power -3, of the mean metal–carbon distances is 1.63.

4. $M_3M'C$ Perovskite Carbides

In these carbides, each M atom has two carbon nearest neighbors at a distance slightly less than 2 Å. The next nearest neighbors are at distances of the order of 4.4 Å and will be neglected. Some Mössbauer spectra, such as those of Fe_3AlC_x, Fe_3GaC_x $(x < 1)$ are complicated by supplementary broad lines related to the nonstoichiometry of these carbides (*7*). All the measured quadrupole splittings lie around 1.5 mm/sec, a large value generally not encountered for compounds presenting a metallic behavior. It seems that the electric field gradients are similar on ^{57}Fe and ^{55}Mn in Mn_3GaC and Mn_3ZnC (*7*, *8*, *18*). The perovskite carbide Fe_4C does not exist. However, regions of ordered Fe_4C were assumed to result from the aging of iron–carbon martensite at room temperature (*19*, *20*). The hyperfine parameters, in the magnetic state, are drawn from a very complex spectrum. The quadrupole splitting of the face-centered iron atoms seems anomalously weak (0.01 mm/sec), except if the easy direction of magnetization is of the [111] type. Finally, the quadrupole splittings of these perovskite carbides do not vary with temperature.

Table VI summarizes the preceding discussion. It gives the iron–carbon (and iron–silicon for Mn_5SiC) distances d less than 2.5 Å and the angle θ(C–Fe–C) of the two shorter iron–carbon bonds for each site. The quadrupole splittings are expected to depend on θ if the two carbon atoms mainly determine their values. The results are presented in the order of increasing θ.

The Mn_2^* site of Mn_5SiC has also been included. The mean iron–carbon distance is 2.25 Å for this site and 2 Å for the ensemble of all the others. A rough estimation Δ^* of the quadrupole splitting which would be obtained if the two carbon atoms were situated at 2 Å is $\Delta^* = 0.71(2.25/2)^3 \simeq 1$ mm/sec. We note finally that a plot of Δ versus $\sin\theta$ leads to the empirical relationship $\Delta_{mm/sec} \simeq 1.5\ (1 - 0.8 \sin\theta)$. A simple point–charge calculation gives the right direction of variation of Δ with θ but, due to its simplicity, not the

TABLE VI

Compound	Iron site	d (Å)	θ (°)	Δ (mm/sec)
Fe_3C	Fe_{II}	2.03–2.04 2.37	99	0.32
Mn_5SiC (^{57}Fe)	Mn_3	2.00–2.06 2.39 (Si)	102	0.28
Fe_5C_2	Fe_{II}	1.98–2.01 2.22	103	0.37
Mn_5SiC (^{57}Fe)	Mn_4	2.02–2.05 2.34(Si)–2.46(Si)	105	0.36
Fe_5C_2	Fe_I	1.97–1.99	142	0.80
Fe_3C	Fe_I	1.97–1.99	144	0.68
Mn_5SiC (^{57}Fe)	Mn_2^*	2.18–2.32	158	0.71
Mn_3GaC (^{57}Fe)	Mn	1.95–1.95	180	1.5
Mn_3ZnC (^{57}Fe)		1.96–1.96		

correct order of magnitude of the ratio $\Delta(180°)/\Delta(90°)$.

Conclusion

The quadrupole splittings of iron atoms having two carbon nearest neighbors, at a distance close to 2 Å, in Fe_3C, Fe_5C_2, Mn_5SiC, and $M_3M'C$ in the paramagnetic state, have been considered. The two strong iron–carbon bonds are responsible for the main part of the observed quadrupole splittings. These quadrupole splittings are nearly independent of the metallic neighborhood of the considered iron sites and increase regularly with the angle of the two iron–carbon bonds. Further confirmations of these conclusions are needed and we will soon study the $(Mn_{1-x}Fe_x)_7C_3$ solid solution.

Acknowledgments

We thank Dr. Spinat for useful information about the anisotropic temperature factors he has measured in Mn_5SiC and Dr. McRae for correcting the English.

References

1. G. Le Caer, J. M. Dubois, and J. P. Senateur, *J. Solid State Chem.* **19**, 19 (1976).
2. P. Spinat, Thèse d'Etat, Universite de Paris VI (1971).
3. P. Spinat and P. Herpin, *Bull. Soc. Fr. Mineral. Cristallogr.* **99**, 13 (1976).
4. P. Spinat, R. Fruchart, M. Kabbani, and P. Herpin, *Bull. Soc. Fr. Mineral Cristallogr.* **93**, 171 (1970).
5. J. Waser, *Acta Crystallogr.* **8**, 731 (1955).
6. R. Fruchart, *Bull. Soc. Chim.*, 2652 (1963).
7. F. Grandjean and A. Gerard, *J. Phys. F.* **6**, 451 (1976).
8. J. P. Senateur, D. Boursier, P. L'Heritier, G. Lorthioir, E. Fruchart, and G. Le Caer, *Mater. Res. Bull.* **9**, 603 (1974).
9. G. Le Caer, A. Simon, A. Lorenzo, and J. M. Genin, *Phys. Status Solids A* **6**, K97 (1971).
10. J. M. Dubois and G. Le Caer, *Acta Met.* **25**, 609 (1977).
11. G. P. Huffman, P. R. Errington, and R. M. Fisher, *Phys. Status Solidi* **22**, 473 (1967).
12. M. Ron and Z. Mathalone, *Phys. Rev. B* **4**, 774 (1971).
13. T. Shigematsu, *J. Phys. Soc. Japan* **37**, 940 (1974).
14. Y. V. Maksimov, I. P. Suzdalev, and R. A. Arents, *Sov. Phys. Solid State* **14**, 2832 (1973).
15. E. Kuzmann, E. Bene, L. Domonkos, Z. Hegedus, S. Nagy, and A. Vertes, *J. Phys. Paris* **C6**, 409 (1976).
16. E. J. Fasiska and G. A. Jeffrey, *Acta Crystallogr.* **19**, 463 (1965).
17. C. Blaauw, F. van der Woude, and G. A. Sawatzky, *J. Phys. C* **6**, 2371 (1973).
18. D. Fruchart, E. F. Bertaut, B. Le Clerc, Le Dang Khoi, P. Veillet, G. Lorthioir, E. Fruchart, and R. Fruchart, *J. Solid State Chem.* **8**, 182 (1973).
19. W. K. Choo and R. Kaplow, *Acta Met.* **21**, 725 (1973).
20. N. De Cristofaro and R. Kaplow, *Met. Trans. A* **9**, 35 (1977).